Crimson Publishers
Wings to the Research

Research Article

Influence of ZnO Nanoparticle Doped Polymer Electrolyte Gel Membranes for H^+ Ion Conduction Based Electrochemical Clean Energy Applications

Neelesh Rai*, Lovely Ranjta* and C P Singh

Department of Physics, AKS University, India

ISSN: 2770-6613

***Corresponding author:** Neelesh Rai and Lovely Ranjta, Department of Physics, AKS University, Satna (MP), 485001, India

Submission: August 01, 2022
Published: August 26, 2022

Volume 4 - Issue 2

How to cite this article: Neelesh Rai*, Lovely Ranjta* and C P Singh. Influence of ZnO Nanoparticle Doped Polymer Electrolyte Gel Membranes for H^+ Ion Conduction Based Electrochemical Clean Energy Applications. Polymer Sci peer Rev J. 4(2). PSPRJ. 000581. 2022.
DOI: 10.31031/PSPRJ.2022.04.000581

Abstract

Proton conducting Nanocomposite Polymer Electrolyte (NCPE) gel membranes based on polyvinyl alcohol-ammonium acetate (PVA-NH_4CH_3COO) and different contents of zinc oxide nanoparticles (ZnO) have been prepared using the solution cast method. SEM image of pure ZnO nanoparticles proves the nanomatric dimension. The OM and XRD analysis revealed that the gel membrane with 0.6wt% ZnO doped NCPE has a high amorphous content and heterogeneous distribution of the constituents. FTIR studies confirmed the complexation between PVA, NH_4CH_3COO and ZnO. The DSC studies prove better thermal behavior upon addition of ZnO nanofiller. Impedance analysis shows that sample with 0.6wt% ZnO nanoparticles has a smaller bulk resistance compared to that of undoped polymer electrolyte. A small amount of ZnO nanoparticles was found to enhance the proton-conduction significantly with two typical maximas; the highest obtainable room-temperature ionic conductivity was $1.22x10^{-3}Scm^{-1}$. Cyclic Voltametry studies reveal that the ionic conductivity is due to the H^+ ion (proton) and their mobility. The highest electrochemical window was recorded at 0.6wt% doped NCPE gel membrane; viz. +5.56V. The availability of H^+ ion (proton) in the system is suitable for the development of eco-friendly rechargeable batteries and fuel cells application.

Keywords: XRD; DSC; Impedance spectroscopy; Nanocomposite polymer electrolytes; H+ ion-conduction; Cyclic voltammetry

Introduction

As described in recent past, the proton-conducting Nanocomposite Polymer Electrolytes (NCPEs) over the past few decades has aimed to provide high-performance and stable electrochemical devices, i.e., electrochemical double-layer capacitors, fuel cells, light-emitting electrochemical cells, smart windows and solid-state batteries [1-4]. The H^+ ion (proton) transport in polymer electrolytes can be chosen based on three mechanisms; hopping, diffusion and transport associated with ion-polymer chain segmental motion [5]. However, the greatest drawback of proton conducting NCPE is their low ionic conductivity at room temperature which restricts their practical applications in energy storage devices [6,7]. Further, Nanocomposite Polymer Gel Electrolytes (NCPGEs) have been given impetus in the electrochemical devices due to certain distinct advantages over solid NCPEs, particularly, ionic conductivity that approaches to that of liquid electrolytes [8,9]. Since nanocomposite polymer gels encapsulate electrolyte solution within the pores, they generally exhibit high ionic conductivity of the order of $\sim 1\times10^{-4}Scm^{-1}$ or more at room temperature [10]. However, in development of such systems, all the processes must be performed in a moisture-free environment as salts in electrolyte solution are highly sensitive to moisture. Another serious problem associated with gel electrolytes is the thermal property of electrolyte at high temperature which may lead to internal short circuit [11]. Therefore, nanocomposite polymer

gel electrolytes do not appear to be viable for commercial device applications, particularly when they are to be deployed under stringent conditions. Also, good mechanical and electrochemical stability of such electrolytes is restricted.

In recent years, significant efforts have been dedicated to enhancing ionic conduction and thermal stability in these protons conducting NCPGEs by different approaches, including polymer blending, copolymerization, addition of plasticizers and incorporation of nanosized inorganic fillers to the system such as carbon nanotubes and metal oxide [7,11,12]. Among these approaches, the dispersion of a small amount of inorganic nano-sized fillers into the polymer electrolyte matrix has captured increasing interest by many researchers due to their high efficiency in improving the room-temperature ionic conductivity as well as maintaining high electrochemical window stability of an electrolyte system [13,14]. Zinc oxide (ZnO) nanoparticles are wide-bandgap semiconductors that possess optoelectrical characteristics. ZnO nanoparticles have been dispersed into numerous solid polymer electrolytes systems to improve the ionic conductivity, structure and mechanical properties of the formed Nanocomposite Solid Polymer Electrolytes (NSPEs) reported earlier [15]. Zebardastan et al. [16] investigated the properties of NSPEs, which consisted of different weight percentages of ZnO nanofiller in the PVdF-HFP:PEO:EC:PC:NaI:I_2:ZnO system. The highest value of ionic conductivity was recorded when ZnO nanofiller was added into the system. They ascribed the enhancement in ionic conductivity to the increase in the amorphous portion in the system.

Recently, Selvi et al. [17] considered the effect of ZnO nanoparticles content on the optical, electrical, mechanical and thermal properties of pure PVA. Based on our recent published works [12,13] the proton-conducting NCPGE based on PVA loaded with NH_4SCN and NH_4CH_3COO exhibits a maximum ionic conductivity of $5\times10^{-4}Scm^{-1}$ at ambient temperature. Although the ionic conductivity and electrochemical stability of this NCPGE is enhanced, it is still insufficient for practical applications. Similar approach has been adopted in the present work; different contents of ZnO nanoparticles were dispersed in the proton-conducting PVA-NH_4CH_3COO nanocomposite polymer electrolyte gel membranes to improve thermal and electrochemical window stability with enhanced ionic conductivity. The samples were prepared by a common solution cast technique and their properties with different ZnO nanoparticles contents were compared. The prepared samples were characterized by impedance spectroscopy, thermal and electrochemical measurements.

Experimental

In the present investigation, PVA (average molecular weight: 124, 000-186, 000; Aldrich make), hydrolysis degree of PVA is greater than 99%. Moreover, PVA is a biodegradable and non-toxic as well as solvent swollen type polymer. Ammonium acetate (NH_4CH_3COO), AR grade and aprotic solvent Dimethyl Sulphoxide (DMSO) were used for synthesis of composite gel membranes. ZnO nanopowder used in the study was obtained from Aldrich, CAS Number: 1314-13-2, purity >97% possessing average particle size smaller than 50nm. PVA (5wt%) was dispersed in 1M salt solution of NH_4CH_3COO in DMSO to form pristine gel electrolyte (DMSO-PVA-NH_4CH_3COO). Subsequently, Nanocomposite Polymer Gel Electrolytes (NCPGEs) viscous solutions were prepared by admixing ZnO nano particles in pristine gel electrolyte solution in different weight proportions followed by thorough mixing at slightly elevated temperature on a magnetic stirrer for seven hours. The so formed solutions were poured in PC pettridishes and covered with Al-foils to avoid contamination and obtain the solvent free standing gel membranes of NCGPEs (Figure 1A). The synthesized NCPGEs have been distinguished with the help of different experimental probes to ap¬praise their performance for device applications. The surface morphology of the pure ZnO nanoparticle was observed using a JEOL scanning electron microscope (Model JSM-6390A) and its different nanocomposite polymer gel electrolytes were observed by using Optical Microscope (OM) with computer-controlled Carl Ziess-Germany make (model HAL-100). Structural morphology and crystal size of pure ZnO nanoparticles were studied by X-ray Diffractometer (model no. RIKAGU, JAPAN MINIFLEX-II) for different nanocomposites polymer electrolytes. The Infrared (FTIR) spectra were sketched on Bruker Alpha platinum ATR Spectrophotometer in a range 4,000-600cm^{-1} at room temperature to completely understand the interaction among the constituents.

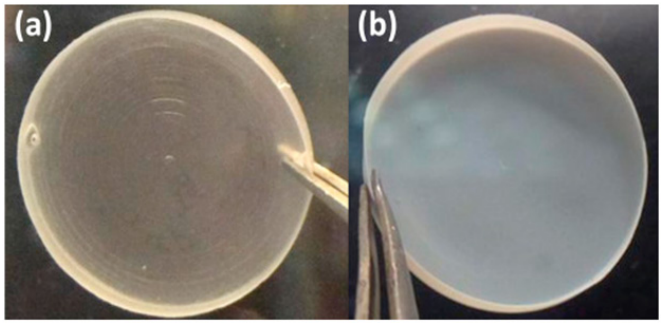

Figure 1A: Free standing gel membranes of PVA-NH_4CH_3COO polymer gel electrolytes without ZnO filler (a) and with 0.5wt% ZnO filler (b).

For thermal behavior of the NCPGEs, Differential Scanning Calorimetry (DSC) was carried out on a NETZSCH DSC model STA449F1 in the temperature range RT to 340 °C at a heating rate 3 °C/min under N_2 environment. Cyclic Voltammetry and Linear Sweep voltametry measurements were recorded using an Electrochemical Analyzer (CH Instruments, USA model no. CHI608D) in the voltage sweep range ±3V keeping the scan rate at $0.1Vs^{-1}$ to assess electrochemical stability and improvement in window as well as confirmation of presence of H^+ ion (proton) in the gel membranes. Complex-impedance spectra were performed in the frequency range varying from 1Hz–1MHz at various temperatures ranging between 35 °C to 98 °C.

Results and Discussion

Surface morphological studies

Figure 1B(a) depicts the SEM image of pure ZnO nano powder.

Granular structure is observed covering the entire surface which can be ascribed; most of the grains of ZnO powder are homogeneous with an individual particle size approximately 50nm. However, some of the irregular particle distribution and agglomeration indicates that ZnO particles are confirmation in to high surface energy of nano particles. Figure 1B(b-d) shows Optical Micrographs (OM) of NH_4CH_3COO: PVA electrolyte membranes containing 0, 0.3 and 0.6 wt% concentration of ZnO. OM image of unfilled PVA gel electrolyte illustrates a microporous structure filled up of PVA chains Figure 1B(b) which was reported earlier [18]. The appearance of pores might be due to the interconnected network of polymer which is created due to solvent evaporation. Addition of 0.3wt% and 0.6wt% ZnO nano particles diminishes the porosity of PVA composite electrolyte because ZnO nanoparticles are captured between chains in the pores Figure 1B(c,d). Also, the pores of small dimension were observed in optical images with relatively homogeneous distribution of pores at still higher concentration of nanoparticles. This supports better solvent retention capability of system. It seems that there exists better compatibility among polymer components in the presence of filler ZnO system.

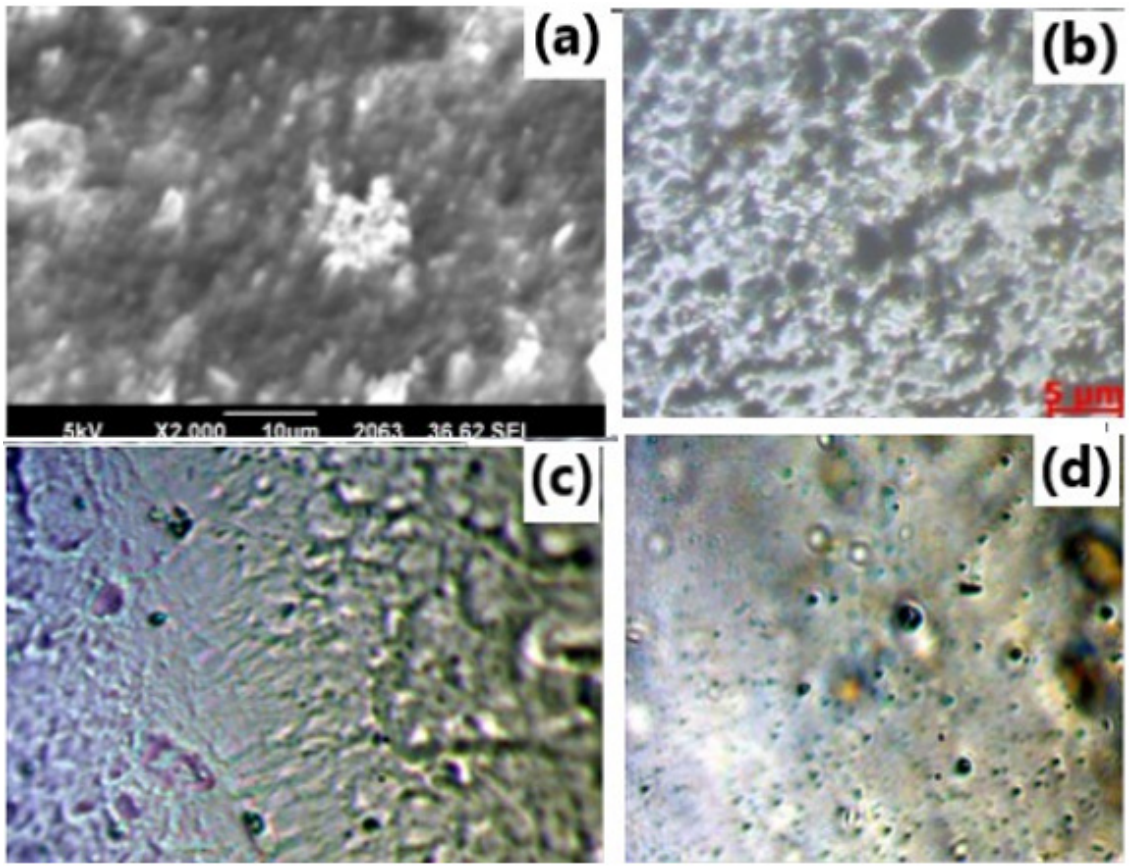

Figure 1B: SEM micrograph of: (a) pure ZnO nanoparticle and OM micrographs of PVA-NH_4CH_3COO with (b) 0.0wt% (c) 0.3wt% (d) 0.6wt% ZnO doped nanocomposite polymer gel electrolyte membranes.

X-ray diffraction studies

The XRD patterns of polymer gel electrolytes membranes of NH_4CH_3COO: PVA without and with ZnO nanofillers along with pristine materials are shown in Figure 2(a-d). The XRD pattern 'inset diffractogram' comprises of crystalline strong peaks of pure ZnO at 2θ=31.78° (100), 33.9° (002), 36.8° (101), 47.63° (102), 56.67° (110), 62.94° (103), 67.98° (112) crystal planes reflecting pure crystalline structure. Comparison of this XRD data with JCPDS (Card No. 36-1451) data reveals hexagonal wurtzite structure with lattice constants a=b=0.324nm and c=0.521nm and no characteristic peaks were observed other than ZnO [19]. In diffraction pattern of without adding filler i.e. PVA-NH_4CH_3COO-DMSO gel membrane (curve-a), apart from background modulation, two relatively intense peaks at 9.3° and 20.2° with combined broadening appear and correspond to characteristics peak of polycrystalline PVA-DMSO complex and membrane exhibits salt NH_4CH_3COO in PVA matrix [8]. Upon addition of 0.3wt% ZnO nanofiller, the peak broadens up and shifts toward higher 2θ values (pattern b&c). This broadened peak might be related to PVA-NH_4CH_3COO-ZnO complex; appears on account of interaction of electrolyte with ZnO leading to formation of nanocomposite as this doesn't correspond to any of the pristine materials; PVA, ZnO and NH_4CH_3COO. Further this broadened peak shifts towards lower 2θ values (pattern d) on increase of ZnO content upto 0.6wt% in NCPGE which reflects complete absorption of ZnO particles in the PVA matrix/enhanced intercalation of dispersoids in matrix electrolyte. This again possibly results from physical interaction among constituents (polymer and salt) in the presence

of filler [14]. The average particle size of the gel membrane was found to be 31nm which is derived from the FWHM of more intense peak located at around 200 using Scherrer's formula (Table 1) and degree of crystallinity (χ_c) of the gel membranes with respect to ZnO was estimated to ascertain improvement in amorphous nature [14] presuming ZnO to be fully crystalline (Table 1) and observed that it decreases with increase in filler concentration which again ascertains change in system morphology on addition of filler.

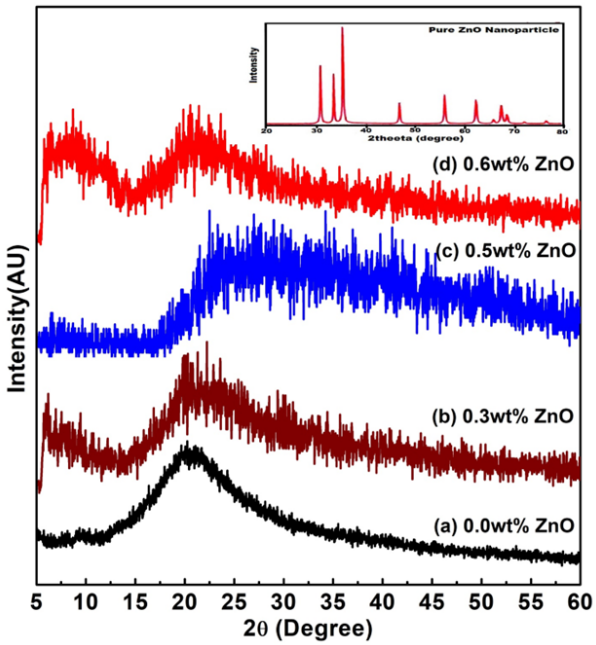

Figure 2: XRD plot for [PVA-NH_4CH_3COO: ×wt% ZnO] NCPGEs with different ZnO nanoparticles: (a) 0.0wt% (b) 0.3wt% (c) 0.5wt% (d) 0.6wt%. The inset diffractogram represents the XRD peaks of pure ZnO nanoparticles.

Table 1: Average crystallites size, degree of crystallinity (χc) and ionic transference number of NCPGEs [PVA-NH_4CH_3COO: ×wt% ZnO] system.

Concentration of ZnO Contents	Average Crystallites Size (nm)	Crystallinity χc (%)	Ionic Transference Number t_{ion}
0 wt%	~ 136	66.2	0.93
0.3 wt %	~ 59	53	0.95
0.6 wt%	~ 31	41	0.98
0.8 wt%	~ 78	63	0.97

FTIR studies

Figure 3(a & c) depict the IR spectra traced for pristine materials and its composite Figure 3(b,d-g) in transmittance mode and the identified transmittance peaks with possible assignments have been listed in Table 2. IR spectra of PVA:DMSO Figure 3(b) reveals the presence of additional absorption peak at wave numbers 702, 1362, 1375, 1418cm^{-1} which are not present in spectra related to pure PVA in Figure 3(a) and DMSO indicating strong interaction among components and correspond to formation of PVA:DMSO complex [8]. Shifting of 702, 843, 1436, 1643 and 2939cm^{-1} peaks towards higher wave number upon addition of NH_4CH_3COO due to interaction with PVA and DMSO further reflects formation of PVA:NH_4CH_3COO-DMSO complex Figure 3(d). The broad absorption peak from 414 to 1339cm^{-1} in FTIR spectra of pure ZnO (inset image) is attributed to the characteristic absorption band of ZnO reported by Shamhari et al. [20]. Besides existence of absorption peaks at 3417, 1557 and 1402cm^{-1} also relates to characteristic band frequencies of ZnO, which are not present in the spectra related to pristine electrolyte i.e., reflecting strong interaction of ZnO with pristine electrolyte and the shifting of the characteristic peak of pristine electrolyte from 3372cm^{-1} to 3327cm^{-1} indicates intercalation of ZnO in the PVA matrix electrolyte. Peaks at 1406, 1317, 706, 619cm^{-1} related to NH def. vib, CH def. vib, asym and C-H wagging mode respectively weaken due to increase in amorphousness of the system on addition of filler. Doublet peaks at 2942cm^{-1} and 2920cm^{-1} related to methyl C-H stretch in pristine gel electrolyte shifted towards lower wave number with broadness and tend to convert in a single peak after addition of ZnO filler in the PVA matrix electrolyte on account of salt-filler-polymer interaction. The continued existence of these variations recommends complex formation of PVA-NH_4CH_3COO and PVA-NH_4CH_3COO-ZnO which have also been seen throughout XRD studies. It is apparent that ZnO acts as active filler in PVA matrix, which dynamically changes the morphology of the structure.

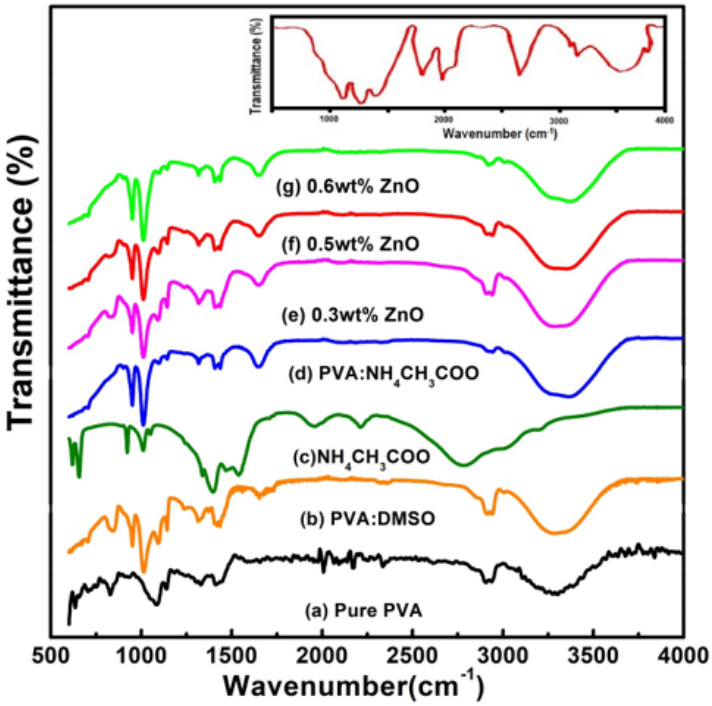

Figure 3: FTIR spectra for [PVA-NH_4CH_3COO: ×wt% ZnO] NCPGE membranes reinforced with different ZnO nanoparticles concentrations: (a) pure PVA (b) PVA-DMSO (c) NH_4CH_3COO (d) PVA:NH_4CH_3COO (e) 0.0wt% (e) 0.3wt% (f) 0.5wt% (g) 0.6wt%. Inset image demonstrations FTIR spectra of pure ZnO nanoparticle.

Table 2: IR transmittance band (in wavenumbers) of Nanocomposite polymer gel membranes [PVA-NH_4CH_3COO: ×wt% ZnO] system.

Descriptions of Vibrations Mode	PVA	PVA:DMSO	NH_4CH_3COO	[(PVA-NH_4CH_3COO): ZnO] System			
				0.0wt%	0.3wt%	0.5wt%	0.6wt%
C H out of plane deformation	714	702	618 657	619 706	608 706	668 702	668 704
Skeletal C-H rocking mode	829	843		906	842	902	902
O-H bending mode	923	951		951	949	952	949
Out of plane N-H bending			922				
C-H wagging mode		1013	1014	1006	1008	1009	1013
C-O stretching mode	1083	1094	1046	1095	1089	1089	1087
C-C and C-O stretching mode of doubly	1135	1141		1139	1140	1143	1144
C-O stretching mode	1236		1244		1234	1234	
CHOH bending mode CH_3 in plane deformation and C C-H wagging mode	1326	1317		1317	1315	1316	1317
CH_3 bending mode			1338		1376		1339

N-H deformation and asymmetric CH_3 bending mode		1362 1375	1401				
C-H deformation mode	1410 1445	1406 1418 1436		1406 1439	1408 1436	1408 1434	1409 1442
N-H bending mode			1471 1539				
C-H stretching	1643			1650	1647	1643	1653
-CONH- bending mode	1661	1659					
C=O stretching mode			1734				
C-H symmetric stretching mode of CH_2 group	2845 2906 2937 3059	2913 2939 3006	2209 2790 3008	2920 2942 3014	2904 2941 3004	2908 2938 3010	2853 2919 2941 3007
O-H stretch	3295	3288	3210	3372	3303	3327	3377

Thermal studies

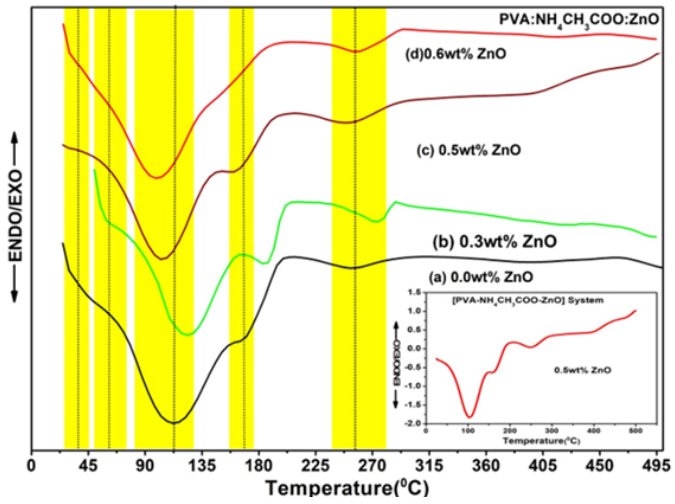

Figure 4: DSC thermograms of [PVA-NH4CH3COO: ×wt% ZnO] system with: (a) 0.0wt% (b) 0.3wt% (c) 0.5wt% (d) 0.6wt% ZnO doped NCPGE membranes. Inset image displays DSC spectra of 0.5wt% ZnO filled NCPGE with presenting heat flex values.

Table 3: Different transition temperature peaks in thermograms of NCPGEs [PVA-NH4CH3COO:×wt% ZnO] system.

[PVA-NH4CH3COO:×wt% ZnO]					
wt% ZnO	P_1	P_2	P_3	P_4	P_5
0	31.2	69	113.21	167	261.22
0.3	35	63.24	102.7	165	261
0.5	31	-	100.49	159.21	250
0.6	31	-	90.73	-	256

Figure 4(a-d) shows the DSC thermogram for (PVA-NH_4CH_3COO: ZnO) system for different filler concentrations. Various thermal transitions noticed in the DSC pattern for NCPGEs under the study are shown in Table 3 (in peaks P_1-P_5). The shift in glass transition temperature and melting temperature with composition (see in Table 3) can be related to the flexibility of polymeric backbone which intern affects conductivity behavior [8,9,21]. Close study of DSC scans (Figure 4) did not reveal any thermodynamics transition in the range 195 °C-250 °C related to melting transition of PVA of a system which reflects complete interaction of polymer component with salt leading to formation of new materials with improved thermal stability. This is observed from DSC scanning in nanocomposite polymer gel electrolyte samples which follow a broad endothermic transition in the temperature range 90 °C-145 °C. The broadness in the transition can be associated to evaporation

of water formed during interaction of PVA with DMSO, the existence of melting transition of ammonium acetate salt (100 °C-114 °C) and presence of gel formation [8,22]. It is further observed in thermogram of the gel membranes that a broad shoulder transition related to complex of polymer salt and filler appears in the temperature range (145 °C-204 °C). Broadness of this transition increases and the melting temperature of polymer electrolyte is observed (around 167 °C) shift towards lower temperature upon addition of ZnO (scan b-d). This is probably due to improve interaction among polymer component in the presence of added salt and filler. Close examination of DSC profile (scan a) shows an endothermic transition in the temperature region around 67 °C is known as glass transition of PVA (around 89 °C; peak P_2) which shift toward lower temperature due to interaction of PVA between salt and polymer [7,8]. Interesting, all the peaks (Table 3) shifted towards lower bands and finally merged in a broad peak on addition of ZnO. This observation indicates improvement in thermal stability in the presence of ZnO filler. The broad peak presence of the third endothermic transition in (240 °C-280 °C) reaffirm improvement in thermal stability of composite system with existence of amorphous nature on addition of ZnO filler particles [9]. Furthermore, Tg is typically calculated in the DSC curve by using a half-height technique in the solid to rubbery state transition region of a polymer. In this region, draw tangent from onset and endset regions and find the value of Tg at the intersecting point of both the tangents.

Conductivity studies

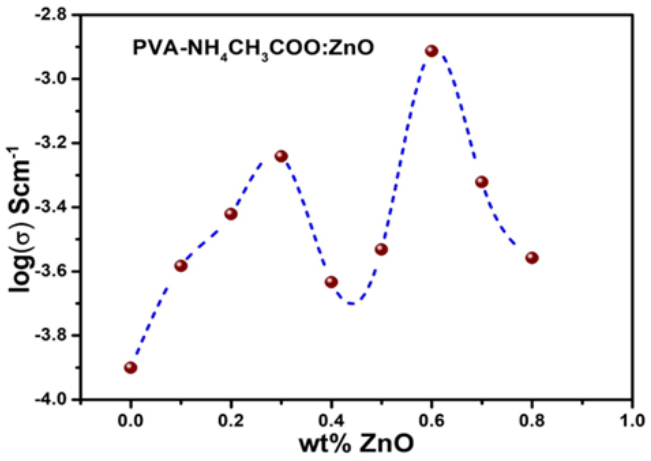

Figure 5: dc conductivity of nanocomposite polymer gel electrolyte membranes with varying concentrations of ZnO nanoparticles.

Figure 5 shows that the conductivity of the gel membranes improves gradually in scale till 0.3wt% and subsequently decreases till 0.4wt% before increasing again (upto 0.6wt%) to achieve an optimum of $\sigma max=1.22\times10^{-3}Scm^{-1}$ and ultimately falling off beyond 0.6wt% ZnO concentration in the NCGPE. Such characteristic is usually observed previously in the polymer nanocomposite electrolyte systems [14]. Consequently, at low filler concentration, greater dissociation of salt and increase in amorphous behavior (also seen in XRD studies) tends to enhance free ions concentration and mobility which significantly improves ionic conductivity. At beyond 0.3wt% filled they serve as cross-linking hub for polymer segments reason immovability of polymer chains in agreement with Tsagarapolous model [23] and thereby reducing the conductivity of the system. The next conductivity maxima is related to formation of highly conducting interfacial layer between ZnO and gel electrolyte caused by filler salt interaction and which ruled over ion-pairing effect. Further, Ranjta et al. [13,14] have recently reported the effect of $BiNiFeO_3$ and Al_2O_3 nano particles variation on ionic conductivity of (PVA-NH_4CH_3COO:×wt%$BiNiFeO_3/Al_2O_3$) gel electrolyte systems. They have revealed that complex formation takes place in the system which tends to raise the conductivity of the system through greater dissociation of salts in the presence of filler.

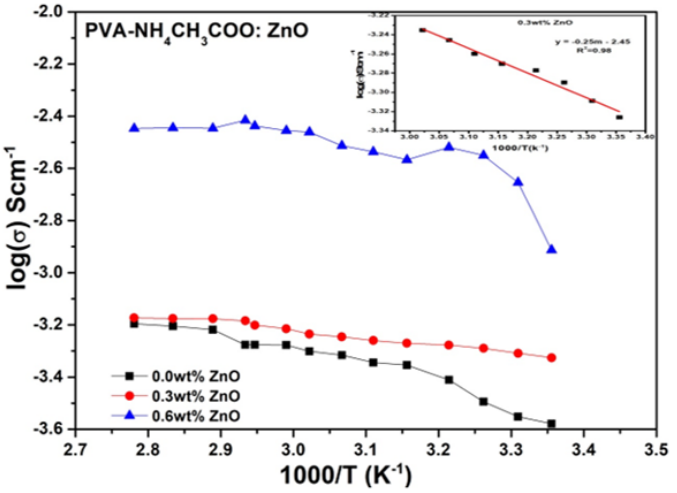

Figure 6: Variation of temperature dependence ionic conductivity of [PVA-NH_4CH_3COO:×wt% ZnO] nanocomposite polymer gel electrolytes membranes with 0.0, 0.3 & 0.6 wt% concentrations of ZnO nanoparticles. Inset image shows conductivity plot of 0.3wt% ZnO filled NCPGE with using linear curve fitting in Arrhenius region for activation energy calculation.

The temperature dependence of ionic conductivity of the NCPGE gel membranes is presented in Figure 6. This shows the increase in conductivity with temperature is attributed to hopping mechanism between coordinated sites, local structural relaxation and segmental motion of the polymer. As the amorphous region progressively increases, the polymer chain acquires faster internal motion and bond rotations (segmental motions). This in turn favors the hopping of inter-chain and intra-chain movement and ionic conductivity of polymer electrolytes become high. Further, it is noticeable from conductivity behavior (Figure 6) that all the curves show two linear regions alienated by a non-linear behavior. The first region (i.e. linear) in the low temperature regime (38 °C to 59 °C), conductivity follows Arrhenius character as described earlier [7,14]. This is probably due to existence of liquid electrolyte encapsulated by the polymer matrix. The high temperature regime (59 °C to 88 °C) conductivity response can be well explained by VTF correlation. As a result, all the curves exhibit a combination of Arrhenius and VTF nature. Moreover, the activation energy (see

Table 1) and other parameters are described by the following Arrhenius relation:

$$\sigma = \sigma_0 T^{-1} \exp(-E_a/kT) \quad \text{..... (1)}$$

where, σ_0 is the pre-exponential factor of conductivity and E_a is the activation energy.

On solving this equation, we can find easy calculation as following

$$\text{Thus, } E_a = 0.08625 \times slope(eV) \quad \text{..... (2)}$$

Subsequently, the value of slope is found easily by applying linear curve fitting in Arrhenius region only also shows in inset image of Figure 6.

Dielectric studies

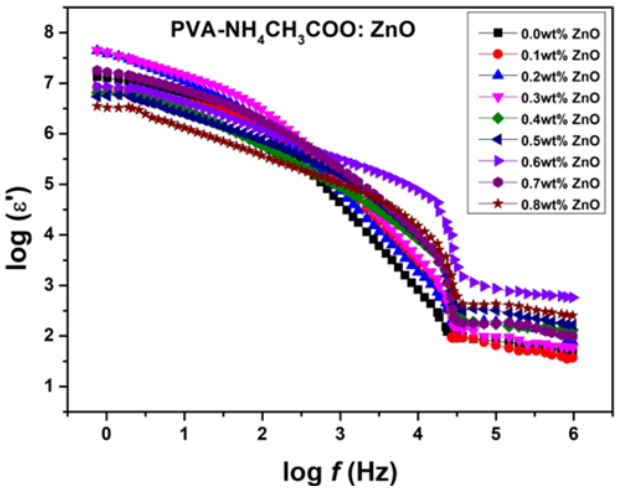

Figure 7a: Variation of dielectric permittivity (ε′) with frequency for [PVA-NH_4CH_3COO: ×wt% ZnO] NCPGEs at room temperature.

Variation of dielectric permittivity (e′) and dielectric loss (e′′) for the different membranes of NCPGE system investigated as a function of frequency at room temperature are shown in Figures (7a & 7b) respectively. Figure 7a shows strong frequency dispersion of permittivity in low frequency region followed by saturation like behavior. This behavior is due to the fact that at low frequencies the dipoles or ionic charges have sufficient time to align with the field before it changes its direction and consequently the dielectric permittivity is high. Whereas the decrease in permittivity value with increasing frequency is attributed to insufficient time for dipoles to align before the field changes direction [24] i.e., inability of dipoles to rotate rapidly leading to a lag between frequency of oscillating dipoles and that applied field. Upon increasing ZnO filler content in the NCPGEs, saturation point shifts towards higher frequency possibly due to decrease in flexibility of NCPGEs system in the presence of added filler. This type of behavior indicates that initially the filler provides almost constant crystalline domain channels up to 0.6wt% filler and thereafter it starts segregating due to non-complexation in PVA-NH_4CH_3COO matrix and it generates uncomplexed dipolar domains in the matrix. High values of dielectric loss (e′′) in low frequency regime (Figure 7b) reflecting the reorientation process of the dipoles in polymer chains which give rise to relaxation peak in dielectric loss spectra. The appearance of a broad peak in the frequency range (10Hz-1KHz) is attributed to the relaxation phenomenon of polymer chain segments [25]. Continuous fall in e′′ values with increasing filler concentration results from attachment of filler with PVA chain through strong interaction among constituents thereby causing transient cross links. These cross links inhibit relaxation of dipoles even at low frequencies which paves way for decrease in dielectric loss values.

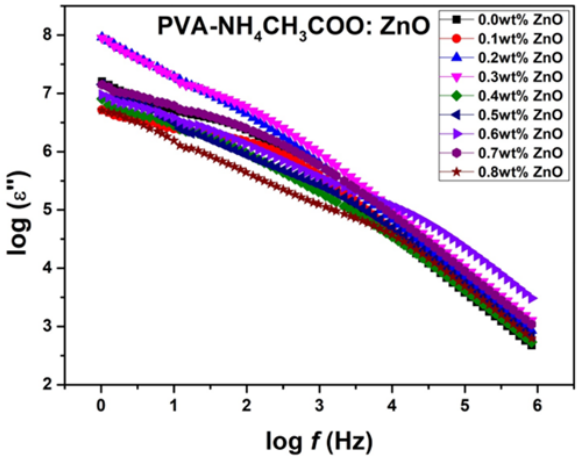

Figure 7b: Variation of dielectric loss (ε′′) with frequency for [PVA-NH_4CH_3COO: ×wt% ZnO] NCPGEs at room temperature.

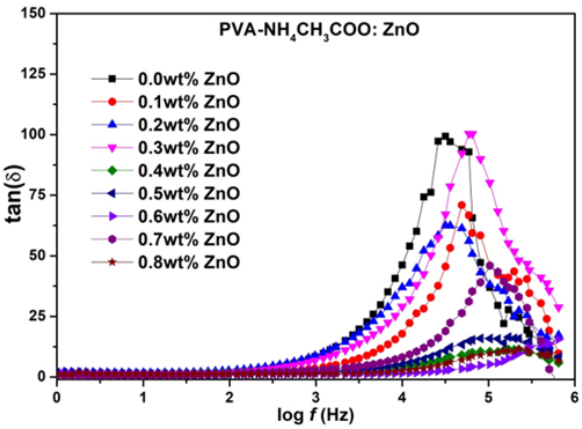

Figure 8: Variation of tanδ vs frequency of NCPGE films for different filler concentrations of ZnO nanoparticles for [PVA-NH_4CH_3COO: ×wt% ZnO] system at room temperature.

Figure 8 shows the plot of tanδ versus frequency of NCPGE membranes for different filler concentrations at room temperature. Dielectric loss tangent is basically the ratio of real and imaginary part of dielectric permittivity discussed earlier [13]. In the Figure 8 change of slope is observed in 3-5KHz frequency range. Essentially such a change correspond to occurrence of a broad peak with system optimizes the presence of scaling dipole and related to the PVA. The maxima of tanδ shifted towards higher frequency and the

height of the peak increased with increasing filler contents. This is due to the increment in number of charge carriers for conduction which decreases the resistivity of the samples [26]. The relaxation frequency is found to shift towards higher value with increase in the filler concentration. Increase the filler content tends to loosen the segmental packing of PVA polymer chain. Higher value of tangent loss can be attributing to the coupling of ion diffusion with segmental motion of polymer chain of gel electrolyte films. Such a behavior can be successfully explained in terms of dielectric relaxation process associated with the presence of heterogeneities in the gel matrix. The loss tangent peaks appeared in the plot for the gel films infer that the H^+ ion in the sample was more capable in following the change in the direction of applied electric field [27]. The result reaffirm system is one of the best ions conducting system.

Electrochemical studies

The electrochemical stability window (i.e., working voltage range) for an electrolyte is an important parameter to be calculated from their application point of view in ionic devices such as batteries, supercapacitors, smart windows etc. [28]. The working voltage range of a typical composition of the NCPGE membranes for different filler concentrations have been estimated using Linear Sweep Voltameter (LSV) in Figure 9a. The NCPGE film has been electrochemically stable upto 5.56V at 0.6wt% content of ZnO, which is a sufficient range for electrochemical application. Therefore, it can be concluded that impregnation of filler can improve the electrochemical stability of gel electrolytes. Further, rapid ion diffusion is observed which promotes the change accumulation at the interface between electrolyte and electrode [29]. Therefore, more energy would be stored in this surrounding area. More electrons will be left and transported from positive electrode to negative electrode when the ion absorption is increased. Figure 9b depicts the cyclic voltagrams of electrolyte films for different filler concentrations. However, this NCPGE system is fully ionic (Table 1). A single prominent oxidation/reduction peak is noticed in cyclic voltagram of all electrolyte systems, around ±0.5V which is possibly due to H^+ (proton) ion that contributes to the ionic conduction and promotes to make device of clean energy [14].

Conclusion

The key objective behind this study was to investigate the ionic conductivity behavior of PVA based gel polymer electrolytes synthesized with ZnO nanoparticle. The transparent, freestanding gel membranes were prepared successfully using solution casting technique. The OM images show heterogeneous distribution of fillers in nanocomposite electrolyte system and chains of PVA fully covered with ZnO filler. XRD studies reveal the complexation between polymer and salt and also amorphicity has enhanced by admixing nanosized ZnO filler. FTIR spectral studies have established the ZnO serves the role of active filler and causing structural changes in the system. DSC studies show improvement in thermal behavior of the system subsequent to filler particles addition. The ionic conductivity of gel polymer electrolytes is found to increase on increasing concentration of ZnO nanofiller in the polymer matrix. The highest ionic conductivity $1.22x10^{-3}Scm^{-1}$ is achieved at room temperature with the addition of 0.6wt% of ZnO. The temperature dependent ionic conductivity is found to obey the Arrhenius behaviour in the lower temperatures whereas the VTF behavior has been observed for higher temperature region. During dielectric spectroscopic investigations, the low frequency dispersion has been linked to the electrode polarization effect in the polymer electrolyte. Wide electrochemical stability of ±5.56V is achieved on addition of 0.6 wt% ZnO filler and confirms the availability of H^+ ion (proton) in the system suitable for the development of clean energy based rechargeable electrochemical device applications in general and batteries & fuel cells in particular.

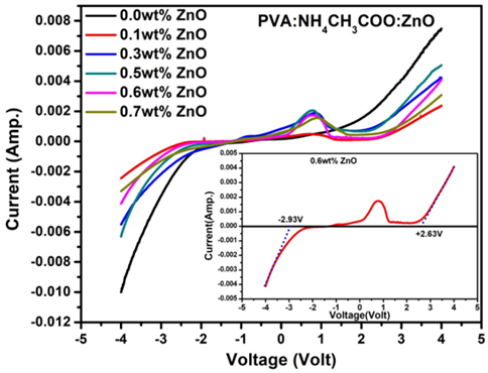

Figure 9a: Linear Sweep Voltammetry (LSV) of [PVA:NH_4CH_3COO:×wt% ZnO] system with varying concentrations of ZnO nanoparticles.

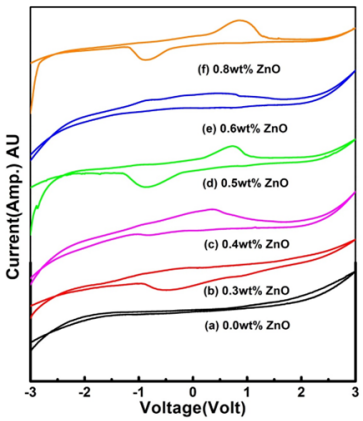

Figure 9b: Cyclic voltagrams of (a) PVA:NH_4CH_3COO gel membranes and its composites containing (b) 0.3wt% (c) 0.4 wt% (d) 0.5 wt% (e) 0.6 wt% (f) 0.8 wt% ZnO nanoparticles.

Acknowledgement

All authors would like to express their gratefulness to the Department of Physics, Pt. Ravishankar Shukla University, Raipur (C.G.) and Dr. Hari Singh Gour University, Sagar (M.P.) for providing the XRD and DSC/TGA analysis respectively for this work.

References

1. Verma ML, Minakshi M, Singh NK (2014) Synthesis & characterization of solid polymer electrolyte based on activated carbon for solid state capacitor. Electrochim Acta 137: 497-503.
2. Hegde S, Ravindrachary V, Praveena SD, Guruswamy B, Sagar RN (2020) Microstructural, dielectric and transport properties of proton-conducting solid polymer electrolyte for battery applications. Ionics 26: 2379-2394.
3. Cheng X, Pan J, Zhao Y, Liao M (2017) Gel polymer electrolytes for electrochemical energy storage. Adv Energy Mater 8(7): 1702184.
4. Wen P, Zhao Y, Wang Z, Lin J, Chen M, et al. (2021) Solvent-free synthesis of the polymer electrolyte via photo-controlled radical polymerization: Toward ultrafast in-built fabrication of solid-state batteries under visible light. ACS Appl Mater Interfaces 13(7): 8426-8434.
5. Patra S, Puthirath AB, Vineesh TV, Narayanaru S, Soman B, et al. (2018) On the development of a proton conducting solid polymer electrolyte using poly (ethylene oxide). Sustain Energy Fuels 2: 1870-1877.
6. Sohaimy MIH, Isa MIN (2017) Ionic conductivity and conduction mechanism studies on cellulose based solid polymer electrolytes doped with ammonium carbonate. Polym Bull 74: 1371-1386.
7. Chand N, Rai N, Agrawal SL, Patel SK (2011) Morphology, thermal, electrical and electrochemical stability of nanoaluminium-oxide-filled polyvinyl alcohol composite gel electrolyte. Bull Mater Sci 34: 1297-1304.
8. Awadhia A, Agrawal SL (2007) Structural, thermal and electrical characterizations of PVA:DMSO:NH_4SCN gel electrolytes. Solid State Ionics 178(13-14): 951-958.
9. Chand N, Rai N, Natarajan TS, Agrawal SL (2011) Fabrication and characterization of nano Al_2O_3 filled PVA:NH_4SCN electrolyte nanofibers by electrospinning. Fibers and Polym 12: 438-443.
10. Stephen AM (2006) Review on gel polymer electrolytes for lithium batteries. Eur Polym J 42(1): 21-42.
11. Choudhary S, Sengwa RJ (2011) Effects of different inorganic nanoparticles on the structural, dielectric and ion transportation properties of polymers blend based nanocomposite solid polymer electrolytes. Electrochim Acta 247: 924-941.
12. Agrawal SL, Rai N (2015) DMA and conductivity studies in PVA:NH_4SCN:DMSO:MWNT nanocomposite polymer dried gel electrolytes. J Nanomaterials 435625: 1-7.
13. Ranjta L, Singh CP, Rai N (2022) Experimental investigations on nano-ferrite embedded nanocomposite polymer electrolytes for proton-conducting rechargeable batteries application. Mater Today: Proceedings 54: 702-709.
14. Rai N, Singh CP, Ranjta L (2022) Structural, thermal and electrical studies of Al_2O_3 nanoparticle soaked electrolyte gel films for novel proton conducting (H^+ ion) eco-friendly device applications. Am J Nano Research and Applications 10(1): 1-8.
15. Xiong HM, Zhao X, Chen JS (2001) New polymer-inorganic nanocomposites: PEO-ZnO and PEO-ZnO-$LiClO_4$ films. J Phys Chem B 105: 10169-10174.
16. Zebardastan N, Khanmirzaei MH, Ramesh S, Ramesh K (2017) Performance enhancement of poly (vinylidene fluoride-cohexafluoro propylene)/polyethylene oxide based nanocomposite polymer electrolyte with ZnO nanofiller for dye-sensitized solar cell. Org Electron 49: 292-299.
17. Selvi J, Parthasarathy V, Mahalakshmi S, Anbarasan R, Daramola MO, et al. (2019) Optical, electrical, mechanical and thermal properties and non-isothermal decomposition behavior of poly(vinyl alcohol)–ZnO nanocomposites. Iran Polym J 29(5): 411-422.
18. Saeed MAM, Abdullah OG (2020) Effect of high ammonium salt concentration and temperature on the structure, morphology, and ionic conductivity of proton-conductor solid polymer electrolytes based PVA. Membranes 10(10): 262-277.
19. Abdullah KA, Awad S, Zaraket J, Salame C (2017) Synthesis of ZnO nanopowders by using sol-gel and studying their structural and electrical properties at different temperature. Energy Procedia 119: 565-570.
20. Shamhari NM, Wee BS, Chin SF, Kok KY (2018) Synthesis and characterization of zinc oxide nanoparticles with small particle size distribution. Acta Chimica Slovenica 65(3): 578-585.
21. Agrawal SL, Shukla PK (2000) Structural and electrical characterization of polymeric electrolytes: PVA-NH_4SCN system. Indian J Pure & Appl Phys 38: 53-61.
22. Agrawal SL, Awadhia A (2004) DSC and conductivity studies on PVA based proton conducting gel electrolytes. Bull Mater Sc 27: 523-527.
23. Agrawal SL, Rai N, Natarajan TS, Chand N (2013) Electrical characterization of PVA-based nanocomposite electrolyte nanofibre mats doped with a multiwalled carbon nanotube. Ionics 19: 145-154.
24. Buraidah MH, Teo LP, Majid SR, Arof AK (2009) Ionic conductivity by correlated barrier hopping in NH_4I doped chitosan solid electrolyte. Physica 404(8-11): 1373-1379.
25. Leones R, Fernandes M, Sentaninc F, Cesarino I, Lima JF, et al. (2014) Ionically conducting Er^{3+}-doped DNA-based biomembranes for electrochromic devices. Electrochemica Acta 120: 327-333.
26. Majid SR, Arof AK (2007) Electrical behaviour of proton–conducting chitosan-phosphoric acid-based electrolyte. Physica 390(1-2): 209-215.
27. Ramya CS, Selvasekarapandian S, Hirankumar G, Savita T, Angelo PC (2008) Investigation on dielectric relaxation of PVP-NH_4SCN polymer electrolyte. J Non-cryst Solids 354(14): 1494-1502.
28. Wang Y, Song S, Xu C, Hu N, Molenda J, et al. (2019) Development of solid-state electrolytes for sodium-ion battery-A short review. Nano Mater Sci 1(2): 91-100.
29. Nahir TM, Clark RA, Bowden EF (1994) Linear-sweep voltammetry of irreversible electron transfer in surface-confined species using the marcus theory. Analytical Chem 66: 2595-2598.